Hindawi
International Journal of Rotating Machinery
Volume 2019, Article ID 2040637, 9 pages
https://doi.org/10.1155/2019/2040637

Research Article

Dynamic Characteristics of Spur Gear Pair with Dynamic Center Distance and Backlash

Jie Liu, She Liu, Weiqiang Zhao, and Lei Zhang

School of Mechanical Engineering, Shenyang University of Technology, Shenyang 110870, China

Correspondence should be addressed to Jie Liu; starliujie@126.com

Received 26 September 2018; Revised 28 January 2019; Accepted 13 March 2019; Published 11 April 2019

Academic Editor: M. Tariq Iqbal

Effect of dynamic backlash and rotational speed is investigated on the six-degree-of-freedom model of the gear-bearing system with the time-varying meshing stiffness. The relationship between dynamic backlash and center distance can be defined clearly. The nonlinear differential equations of the model are solved by the Newmark-β method. The results show that system amplitude increases in the wake of increasing rotational speed. After reaching a certain rotational speed, the system jumps from periodic motion to chaos motion, and the effective amplitude is changed violently. Comparing the dynamic backlash with fixed backlash, the amplitude of the dynamic backlash is augmented and the frequency components are diversified. The vibration displacement is enlarged by the dynamic backlash and the chaotic behavior of the system becomes complex with increasing rotational speed. The numerical results provide a useful reference source for engineers to select rotational speed section for steady running.

1. Introduction

Gear transmission system is called as one of the most important mechanisms used to transmit power and motion in the modern machinery industry, whose mechanism and complex nonlinear phenomenon have been the focus. The lifetime of gear transmission system is reduced by a series of nonlinear factors and nonlinear excitation, including dynamic backlash, time-varying meshing stiffness, dynamic transmission error, and gear eccentricity. Therefore, it is necessarily analyzed for the dynamic behaviors of the gear transmission system and effect of the parameters on the system. In order to greatly enhance performance, reliability, and dynamic stability of the gear system, the effects of dynamic parameters and excitation have been the focus on research.

Plentiful research achievements have been accomplished by many outstanding scientists. S Theodossiades and S Natsiavas [1] researched dynamic characteristics of gear pair system, including backlash and time-periodic stiffness. Their theory is used to guide later scientists to investigate dynamic characteristics of the gear pair system. L Walha et al. [2] presented a two-stage spur gear system, in which periodically changing stiffness and fixed backlash were both taken into consideration. They indicated that amplitude jumps were generated by fixed backlash. Hamed Moradi and Hassan Salarieh [3] investigated dynamic response of gear system with nonlinear backlash, which is more realistic than constant backlash. The nonlinear backlash function was expressed by a smooth third-order polynomial and oscillatory different equations of the system were solved using the multiple scale method. Wei S et al. [4] proposed a single-mesh gear system to investigate effect of periodic meshing stiffness and backlash nonlinearity based on improved IHBM method.

There scholars have made contributions to research of gear transmission system with nonlinear factors. However, in order to be more tally with the actual situation, more and more scholars developed dynamic factors and the time-varying parameters on gear-bearing system or gear-rotor-bearing system. Cao Z et al. [5] studied dynamic responses in the planetary gear system, in which gear eccentricity was taken into consideration and observed meshing stiffness changes due to the time-varying center distance and gear eccentricity. Lu JW et al. [6] established a dynamic model of the gear transmission system with the stochastic perturbation of parameters. They indicated that motion of the system became more complex due to increasing perturbation intensity. But the unstable motion of the system transformed the

steady periodic motion when the perturbation intensity is considerably great. The extended research of Lu JW et al. [7] established one-stage gear system model, in which stochastic backlash was included. The relationship between stability of system and random backlash was discussed. The dynamic characteristics of the one-stage gear system were influenced by random backlash, and chaotic behaviors of the system could be enlarged due to random backlash. Researching the perturbation of the gear system parameters was made among scholars, and the foundation is provided for further research.

However, some facts are ignored. Some scientists studied considering more factors. Chen Q [8] researched the gear system with fractal theory. The fractal theory was employed to express the dynamic instead of constant backlash. It was clearly generated that the fractal backlash was more reasonable form than fixed backlash and random backlash. The research of the gear system with the fractal characteristics is used to guide the design, manufacture, and choice of the accuracy grade of the gear tooth surface. To further explore dynamic backlash, the time-varying mesh stiffness of a spur gear pair was changed with changing the center distance error, which was developed by Yong L et al. [9]. Chen SY et al. [10] raised a 6-DOF gear meshing model, in which the time-varying mesh stiffness, dynamic backlash, and effect of friction were included. The variation of dynamic meshing force became complex with increasing rotational speed. Xiang L et al. [11] studied the gear transmission model with dynamic friction and dynamic backlash based on the Runge-Kutta numerical method and observed effect of backlash and gear eccentricity under different rotational speeds.

Although some dynamic factors of the gear system are discussed, few researches have investigated the effect of the rotational speed on a dynamic model of the gear-bearing transmission system with dynamic center distance and backlash. In this paper, a 6-DOF dynamic model of the gear-bearing transmission system is established. The coupled relationship between the dynamic backlash and the vibration responses of gear system is researched by analyzing effect of the rotational speed and dynamic backlash variation. The differential equations of motion are solved using the Newmark-β method and the simulation results including 3D frequency diagram and bifurcation figure are described. The dynamic backlash on the system with the center distance error is clearly defined to further develop the gear system running mechanism. And we will focus on effect of the rotational frequency on the multi-degree-of-freedom dynamic gear system. The research provides a reference for selecting appropriate rotational frequency interval with gear system. It is practically significant to ensure the stability of the gear transmission.

2. Dynamic Model of the Gear-Bearing System

2.1. The Lumped Mass of the System. Figure 1 is set to express simplified 6-DOF lumped mass model in the paper. Figure 1 presents schematic diagram of the dynamic system with gears and bearings.

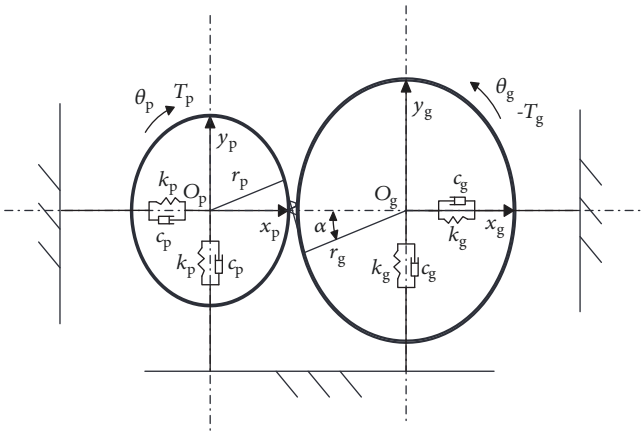

Figure 1: 6-DOF model of the gear-bearing system.

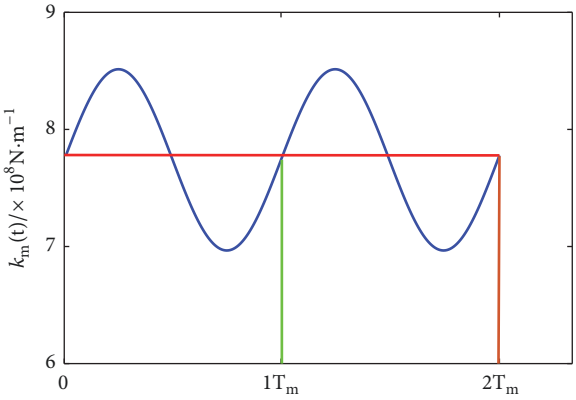

Figure 2: The meshing stiffness.

The nonlinear model of the gear system with gear inertia J_p and J_g, gear masses m_p and m_g, and base circle radius r_p and r_g as shown in Figure 1 is considered here. The symbol θ_j (j=p,g) is the dynamic angular displacements of the gears. The bearings are modeled by elements with viscous damping coefficients c_j (j=p, g) and linear springs k_j (j=p, g). The time-varying meshing stiffness k_m is expressed as [12]

$$k_m(t) = k_m^0 \left[1 + k_m^t(t)\right], \tag{1}$$

where k_m^0 is the averaged tooth stiffness and k_m^t is variant part of the meshing stiffness. The stiffness is shown in Figure 2. Tm is the gear meshing period. The high-frequency internal excitation caused by the static transmission error [13] is written as

$$e_m(t) = e_m^0 \left[1 + e_m^t(t)\right], \tag{2}$$

where $e_m(t)$ is the static transmission error, e_m^0 is averaged static transmission error, and $e_m^t(t)$ is the variant part of the static transmission error. The relative displacement between the pinion and the gear is

$$\begin{aligned}\delta(t) = {} & \left(x_p \sin\psi - y_p \cos\psi + r_p\theta_p\right) \\ & - \left(x_g \sin\psi - y_p \cos\psi + r_g\theta_g\right) - e_m(t).\end{aligned} \tag{3}$$

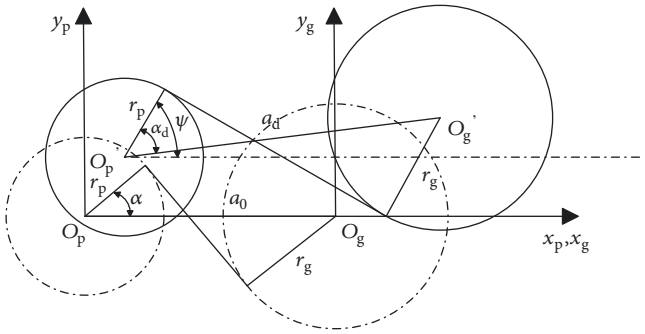

Figure 3: Simplified illustration of dynamic center distance considering gear eccentricity.

The dynamic meshing force acting on the meshing points is

$$F_m = c_m \dot{\delta} + k_m f(\delta), \tag{4}$$

where c_m is the meshing viscous damping coefficient. $f(\delta)$ is the backlash function which will be defined later in the paper.

2.2. The Dynamic Backlash. Figure 3 presents simplified illustration of the dynamic center distance with variation of gear eccentricity. Real circles O_p, O_g and dotted circles O_p', O_g' are, respectively, original position of the gears and the position of the gear system of generating vibration. The new gear axle center coordinates are, respectively, (x_p, y_p) and (x_g, y_g). The actual center distance and the theoretical center distance are denoted by a_d and a_0 as described in Figure 3. The instantaneous distance between the pinion and the gear is expressed as [14]

$$a_d = \sqrt{\left(a_0 - x_p + x_g\right)^2 + \left(y_p - y_g\right)^2}. \tag{5}$$

The dynamic pressure angle is defined as [15]

$$\alpha_d = \arccos \frac{\left(r_p + r_g\right)}{a_d}, \tag{6}$$

where r_p and r_g are the base radius of driving gear and driven gear. The position angle is defined as

$$\psi = \alpha_d + \arcsin \frac{\left(y_g - y_p\right)}{a_d}. \tag{7}$$

Theoretically, the backlash should be zero because the gears are designed without the real situation of the gears running. Actually, in order to avoid seizing after the frictional heating expansion of the gear system and make sure to form lubricating film between the tooth profiles, a backlash must be considered in the gear design. If the center distance is changed, instantaneous backlash will be altered. The graphic about the tooth flanks with backlash is shown in Figure 4. The dynamic backlash is expressed as

$$b_d = b_c + \left(a_d - a_0\right) \tan \alpha_d, \tag{8}$$

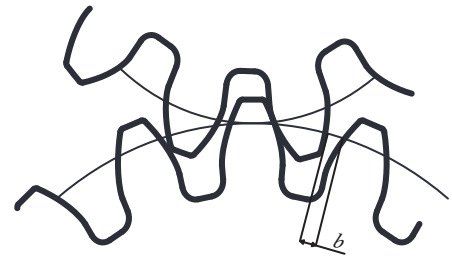

Figure 4: Sketch of backlash.

where b_d is the dynamic backlash and b_c is the backlash. The backlash function of the nonlinear dynamic system can be written as [13]

$$f(\delta) = \begin{cases} \delta - b_d & \delta \geq b_d \\ 0 & |\delta| < b_d \\ \delta + b_d & \delta \leq -b_d. \end{cases} \tag{9}$$

2.3. Equation of Motion. The equations of motion of the gear-bearing system can be expressed as

$$\begin{aligned} m_p \ddot{x}_p + c_p \dot{x}_p + k_p x_p + F_m \sin\psi &= 0 \\ m_p \ddot{y}_p + c_p \dot{y}_p + k_p y_p - F_m \cos\psi &= 0 \\ J_p \ddot{\theta}_p &= T_p - r_p F_m \\ m_g \ddot{x}_g + c_g \dot{x}_g + k_g x_g - F_m \sin\psi &= 0 \\ m_g \ddot{y}_g + c_g \dot{y}_g + k_g y_g + F_m \cos\psi &= 0 \\ J_g \ddot{\theta}_g &= -T_g + r_g F_m, \end{aligned} \tag{10}$$

where r_j (j=p,g) is the base radius of the pinion and gear, respectively. A dimensionless form of Equations (10) is obtained by letting $m_e = J_p J_g / (J_p r_g^2 + J_g r_p^2)$, $\varepsilon_p = m_p/m_e$, $\varepsilon_g = m_g/m_e$, $\lambda_p = k_p/k_m^0$, $\lambda_g = k_g/k_m^0$, $\delta_p^2 = \lambda_p/\varepsilon_p$, $\delta_g^2 = \lambda_g/\varepsilon_g$, $\omega_n^2 = k_m/m_e$, $X_p = x_p/b_0$, $Y_p = y_p/b_0$, $X_g = x_g/b_0$, $Y_g = y_g/b_0$, $U = (r_p\theta_p - r_g\theta_g)/b_0$, $E_m = e_m/b_0$, $\omega_n^2 = k_m^0/m_e$ and $\tau = \Omega t$, where Ω is the meshing frequency. The 5-DOF dimensionless equations of the gear motion are concluded as

$$\begin{aligned} &\Omega^2 \ddot{X}_p + 2\Omega\xi_p\sigma_p\omega_n\dot{X}_p + \left(\sigma_p\omega_n\right)^2 X_p \\ &\quad + \left[2\Omega\xi_m\omega_n\dot{\Delta} + \omega_n^2\left(1 + k_m^t\right) f(\Delta)\right] \frac{\sin\psi}{\varepsilon_p} = 0 \\ &\Omega^2 \ddot{Y}_p + 2\Omega\xi_p\sigma_p\omega_n\dot{Y}_p + \left(\sigma_p\omega_n\right)^2 Y_p \\ &\quad - \left[2\Omega\xi_m\omega_n\dot{\Delta} + \omega_n^2\left(1 + k_m^t\right) f(\Delta)\right] \frac{\cos\psi}{\varepsilon_p} = 0 \\ &\Omega^2 \ddot{X}_g + 2\Omega\xi_g\sigma_g\omega_n\dot{X}_g + \left(\sigma_g\omega_n\right)^2 X_p \\ &\quad - \left[2\Omega\xi_m\omega_n\dot{\Delta} + \omega_n^2\left(1 + k_m^t\right) f(\Delta)\right] \frac{\sin\psi}{\varepsilon_g} = 0 \end{aligned}$$

Table 1: Parameters of the gear-bearing system.

Parameter	Symbol	Numerical value
Pressure angle	α	20°
Moment of inertia	J_1/J_2	0.041/0.079 kg·m^2
Mass	m_1/m_2	1.53/3.01 kg
Stiffness of bearings	k_1/k_2	2/2×10^8 N·m^{-1}
Meshing stiffness	k_m	7.74×10^8 N·m^{-1}
Teeth	z_1/z_2	55/75
Modulus	m	2
Phase angle of meshing stiffness coefficient	φ_k^1	0
Phase angle of the transmission error	φ_e^1	0
Transmission error	e_m^1	1×10^{-5} m
Half-backlash value	b	2×10^{-5} m
Driving torque	T_d	22 N·m
Loading torque	T_l	30 N·m
Meshing damping ratio	ξ_1	0.07
Contact damping ratio	ξ_2	0.07

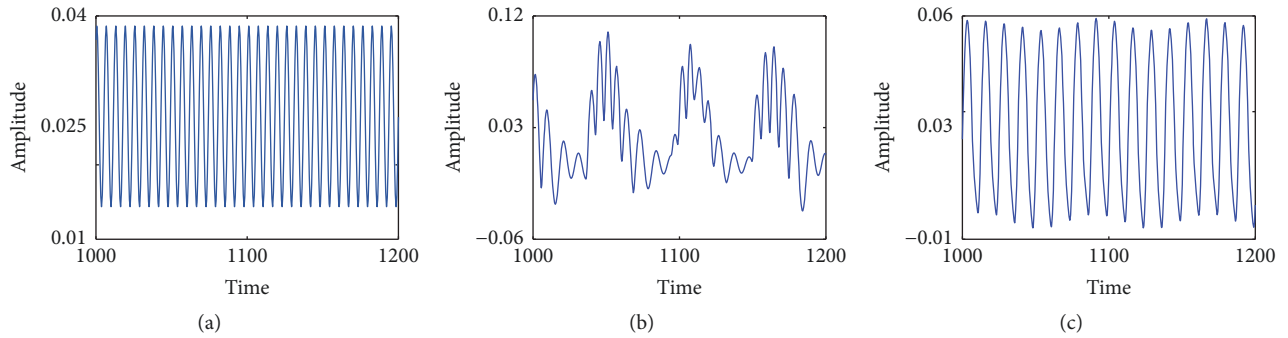

Figure 5: The dynamic backlash variation with different frequency: (a) $\omega = 1$, (b) $\omega = 2$, and (c) $\omega = 3$.

$$\Omega^2 \ddot{Y}_g + 2\Omega\xi_g\sigma_g\omega_n\dot{Y}_g + \left(\sigma_g\omega_n\right)^2 Y_g + \left[2\Omega\xi_m\omega_n\dot{\Delta} + \omega_n^2\left(1 + k_m^t\right) f(\Delta)\right]\frac{\cos\psi}{\varepsilon_p} = 0$$

$$\Omega^2\ddot{U} + 2\Omega\xi_m\omega_n\dot{\Delta} + \omega_n^2\left(1 + k_m^t\right) f(\Delta) = \frac{T_p}{m_e r_p}, \tag{11}$$

where Δ is the dimensionless relative displacement expressed as

$$\Delta(t) = X_p\sin\psi - Y_p\cos\psi - X_g\sin\psi + Y_p\cos\psi + U - E_m(t). \tag{12}$$

3. Results and Discussion

The parameters of gear transmission are listed in Table 1. In this section, in order to explore the nonlinear responses of the gear-bearing transmission system, Eq. (11) with dimensionless equations can be solved using the Newmark-β method. Meshing frequency $\omega = \Omega/\omega_n$ is regarded as the key parameter, which is controlled. In the following analysis, the displacement and amplitude from dimensionless equation will be depicted as shown in 3D frequency diagram, bifurcation spectrum, Poincaré map, and so on.

3.1. Dynamic Backlash and Dynamic Meshing Angle. For the gear system with dynamic backlash, it is first for dynamic backlash and dynamic meshing angle to make comparison with different ω as shown in Figures 5 and 6 because the frequency ω is very significant and a lot of brilliant scientists were devoted to investigating the nonlinear dynamic characteristics of the gear transmission system.

In Figures 5(a), 5(b), and 5(c), the dynamic backlash is steadily on the system with the frequency $\omega = 1$. The dynamic backlash presents serious fluctuation when the frequency ω is 2. With the frequency reaching 3, this fluctuation is decreased. The amplitude is dimensionless.

The dynamic meshing angle of the gear system is shown in Figures 6(a), 6(b), and 6(c) at different frequency severally, including $\omega = 1$, $\omega = 2$, and $\omega = 3$. The characteristics of dynamic meshing angle are similar to the dynamic backlash. To further explore the dynamic backlash and the dynamic meshing angle, we will research the global characteristics of the backlash and angle by using the amplitude-frequency response curve of the dynamic backlash and dynamic

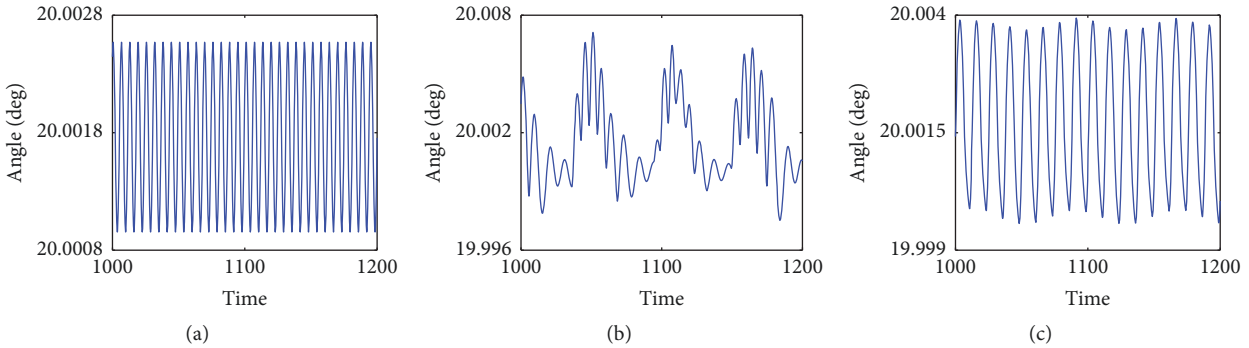

Figure 6: The dynamic meshing angle variation with different frequency: (a) $\omega = 1$, (b) $\omega = 2$, and (c) $\omega = 3$.

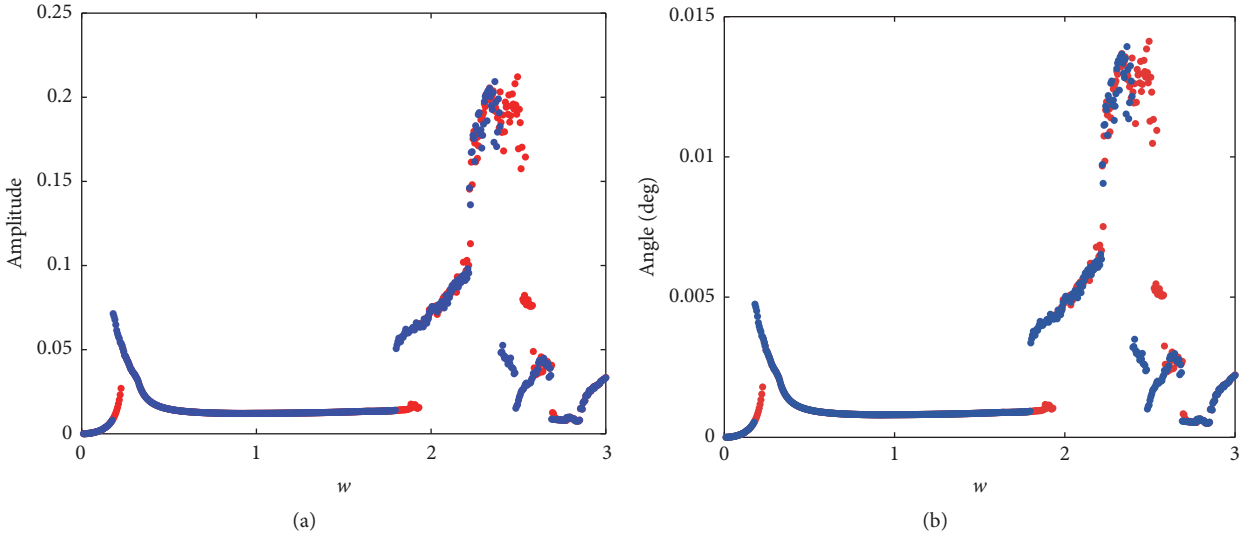

Figure 7: Amplitude variation with respect to frequency: (a) dynamic backlash, (b) dynamic meshing angle, forward sweep frequency (denoted by blue point), and reverse sweep frequency (denoted by red point).

meshing angle with respect to the frequency ω as shown in Figures 7(a) and 7(b), respectively. The amplitude of the backlash and the degree of the meshing angle are both steady values in the range of $\omega \in [0.4, 1.9]$. The increasing and fluctuation present in the range of $\omega \in [1.9, 2.7]$ and values of the backlash and the angle are both shown as fluctuation decrease and small value in the range of $\omega \in [2.7, 3]$.

3.2. Nonlinear Characteristics of Gear System with Constant Backlash. Firstly, for the nonlinear system with constant backlash, meshing frequency ω is controlled and the frequency ω is determined as $\omega = 1$, $\omega = 2$, and $\omega = 3$. The phase diagrams and Poincaré maps are exhibited in Figure 8. It is explicitly illuminated that the motion trail of phase plane becomes more complex with increasing the frequency ω. The amplitude variation of the system is showed as the tendency of inverted parabolic. As shown in Figure 8, T-periodic motion, multi-periodic motion, and chaos motion are described with increasingly dispersing the points in Figures 8(d), 8(e), and 8(f). The phase diagrams and Poincaré maps only express a few parts of the nonlinear characteristics of the gear transmission system. In order to explore more detailed nonlinear responses, bifurcation diagram and 3D frequency spectrum are showed in the following.

3.3. Nonlinear Characteristics of Gear System with Dynamic Backlash. Firstly, for the sake of developing the nonlinear response of the multi-degree-of-freedom model, comparing constant backlash model with dynamic backlash model, the different characteristics are described by bifurcation map and 3D frequency spectrum as shown in Figures 9, 10, and 11. The frequency ω as control parameter is the most important, which is key to explore the dynamic response of the multi-degree-of-freedom system. Detailedly, the same system parameters and numerical method are applied to two different models involving constant backlash model and dynamic backlash model.

Here, the amplitude maps of vibration are showed in Figure 9. The amplitude is dimensionless value. The ω is regarded as varying in the range of $\omega \in [0, 3]$. The amplitude value in torsional direction is expressed as the difference between the highest and the lowest amplitude values, following divided by 2. With the increase of the frequency ω, in Figure 9(a), it can be clearly surveyed that amplitude goes from increasing

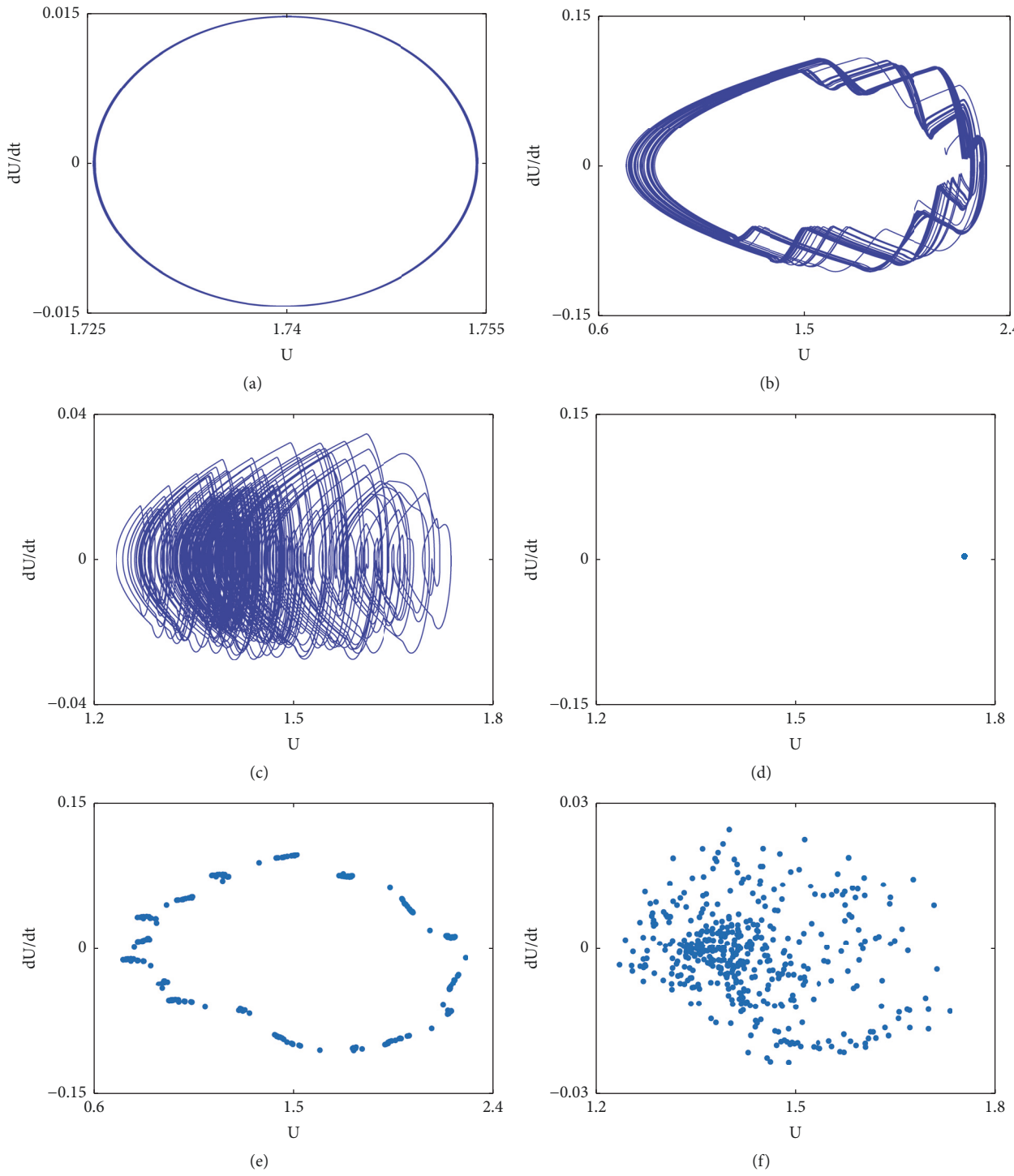

FIGURE 8: The nonlinear characteristics of gear-bearing system with constant backlash. Phase map: (a) $\omega = 1$, (b) $\omega = 2$, and (c) $\omega = 3$; Poincaré maps: (d) $\omega = 1$, (e) $\omega = 2$, and (f) $\omega = 3$.

to the decreasing within the limits of $\omega \in [0, 0.5]$, as the characteristic of amplitude of the constant backlash model at the slow meshing frequency. Subsequently, the tendency of amplitude value verges on stabilization in the range of $\omega \in [0.5, 1.6]$. In addition, the amplitude variation presents an approximate linear characteristic.

Afterword, the tendency causes explosive increase in the range of $\omega \in [1.6, 2.7]$, which is discrete distribution. At $\omega \in [2.7, 3]$, the amplitude further becomes feeble discreteness, and the situation is stability in this range. In Figure 9(b), the nonlinear responses of the system are described. It is obvious that steady amplitude value is shown in the range

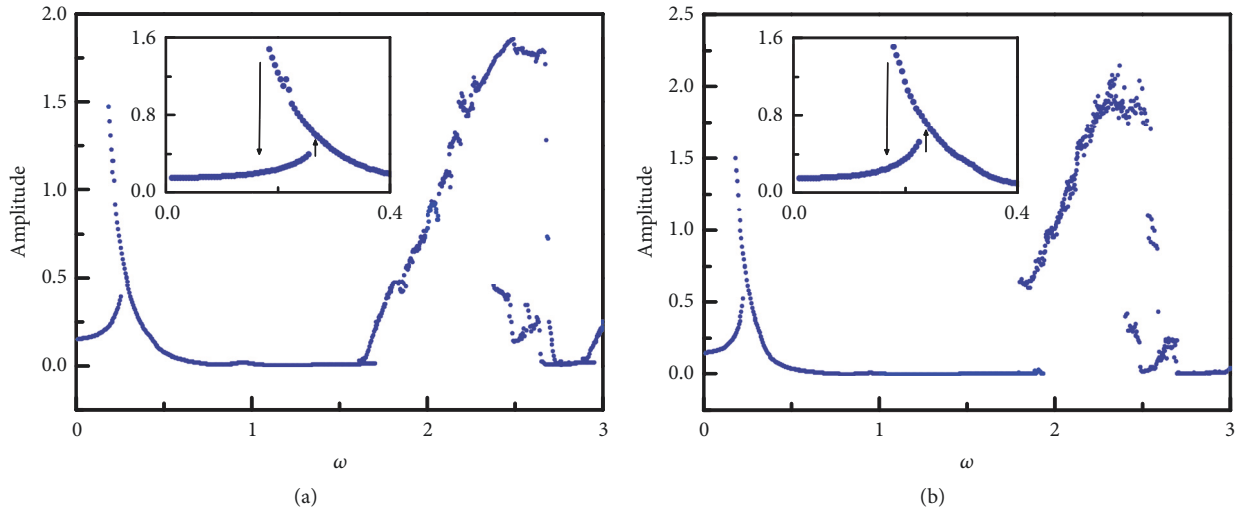

Figure 9: Amplitude vibration of the six-degree-of-freedom system: (a) constant backlash; (b) dynamic backlash.

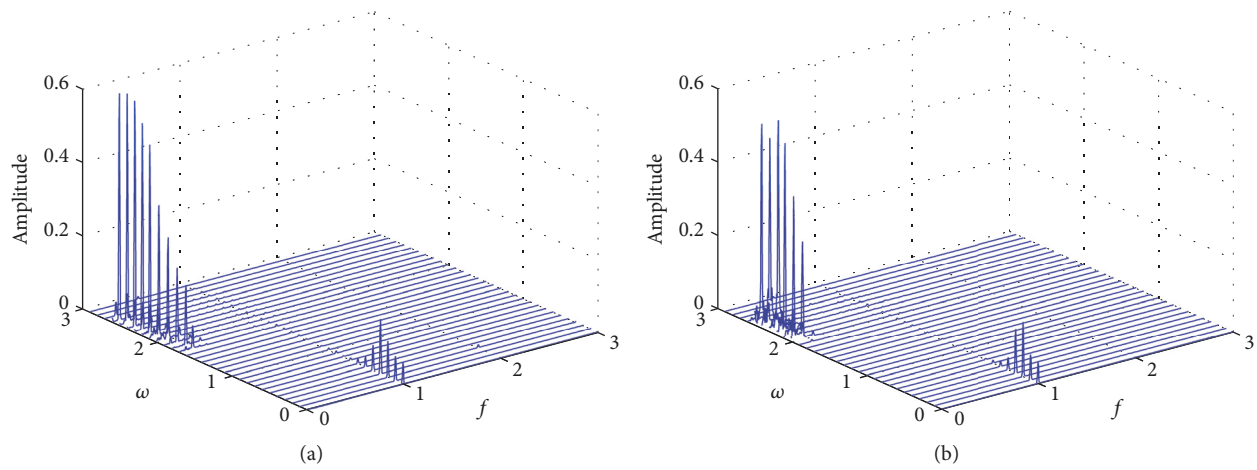

Figure 10: 3D frequency spectrum using ω as the control parameter. (a) Constant backlash and (b) dynamic backlash.

of $\omega \in [0.4, 1.9]$. Then the distribution of points is more complex and discrete than the constant backlash model in the range of $\omega \in [1.9, 2.7]$. According to the above comprehensive analysis, it can be gotten for a matching rotational speed to steadily run. For the stability of the system, the appropriate speed of the system with dynamic backlash is in the range of $\omega \in [0.4, 1.9]$.

In the dynamic model, 3D frequency spectrum diagrams are depicted by Figure 10. The comparison between Figures 10(a) and 10(b) shows that the major frequency amplitude increases with the increase of the frequency ω on the system with constant backlash, and superharmonic and subharmonic frequencies are kind of vague. On the contrary, the major frequency amplitude is more complex and irregular and the frequency component presents diversity in Figure 10(b).

The bifurcation diagram of the system of constant backlash is shown in Figure 11(a). Complex bifurcation and chaos phenomenon about dimensionless relative displacement x_h on meshing point emerged with increasing the frequency ω. As the dimensionless frequency ω is low, the system motion is T-periodic motion in the range of $\omega \in [0, 1.6]$. Then, the system suddenly changes to chaos motion within the limit of $\omega \in [1.6, 2.25]$. Successively, the system undergoes from nT-periodic motion at $\omega \in [2.25, 2.5]$ to quasi-periodic motion at $\omega \in [2.5, 2.6]$ and to nT-periodic motion in the range of $\omega \in [2.6, 2.7]$. Conclusively, through 2-periodic motion in the range of $\omega \in [2.7, 3]$, the system is going to back to chaos motion again.

The bifurcation diagram of the system of dynamic backlash is described in Figure 11(b). The bifurcation behavior of the dimensionless relative displacement of mesh point x_h is obviously reduced. The system motion is from the T-periodic motion, through chaos motion at $\omega \in [1.9, 2.6]$, to the quasi-periodic in the range of $\omega \in [2.6, 2.7]$. Finally, the system behavior is chaos motion again, by 2-periodic bifurcation in the range of $\omega \in [2.7, 3]$. Thus, it can be seen that the type of system motion is simplified by dynamic backlash, involving 1-periodic motion and chaos motion, but chaos motion is more complex and unpredictable than nT-periodic motion.

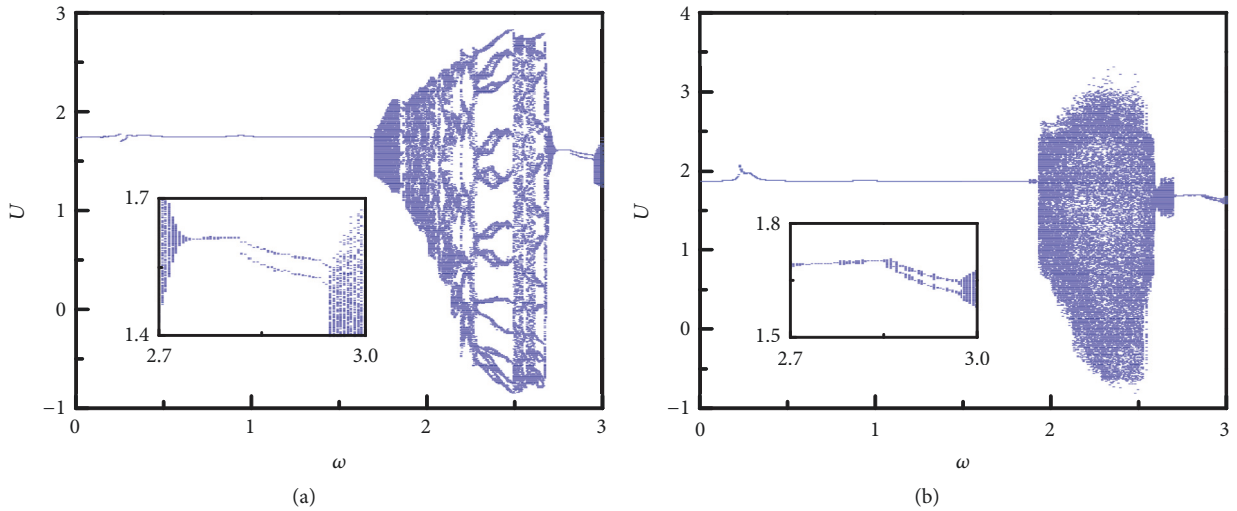

Figure 11: Bifurcation map of vibration displacement U of the six-degree-of-freedom system. (a) Constant backlash and (b) dynamic backlash.

In other words, the system behavior becomes more complex and dynamic backlash can defer the beginning of the chaos motion.

4. Conclusions

In this paper, the nonlinear dynamic model of gear-bearing transmission system is established as the key to explore the nonlinear responses. In detail, the effects of the constant and dynamic backlash on gear-bearing transmission system have been developed. The relationship between gear center distance and the dynamic backlash is defined considering the gear and bearing factors. To adopt by bifurcation diagram, 3D frequency spectrum, and phase diagram, the influence of the frequency ω on the system is explored. The results show the following:

(1) With increasing the frequency ω, the amplitude of the system with dynamic backlash is heightened. In other words, it is observed that vibrational energy between gears becomes bigger. Effect of dynamic backlash on the system amplitude showed that the energy changes and becomes more and more complex.

(2) In 3D frequency spectrum, the amplitude of the system with constant backlash is gradually rising in the wake of increase of the frequency ω. Nevertheless, the amplitude of the system with dynamic backlash becomes very complicated and changeable. Superharmonic and subharmonic of the response are a lot fresher on the system of dynamic backlash than the system with constant backlash.

(3) By means of numerical simulation, bifurcation diagram, phase diagram, and Poincaré map are obtained. With the dynamic backlash, the gear system undergoes from T-periodic motion, through chaos motion, to qusia-periodic motion and back to periodic motion following varying the frequency ω. After synthetically considering conclusions (1) and (2), the most appropriate rotational speed can be identified to ensure that the gear transmission system operates normally.

Data Availability

All the data is in the manuscript. If the researchers are interested in obtaining the numerical solution files, please contact email address: 1274186512@qq.com.

Conflicts of Interest

The authors declared no potential conflicts of interest with respect to the research, authorship, and publication of this article.

Acknowledgments

The authors gratefully acknowledge the financial support provided by Natural Science Foundation of China (No. 51675350).

References

[1] S. Theodossiades and S. Natsiavas, "Periodic and chaotic dynamics of motor-driven gear-pair systems with backlash," *Chaos, Solitons & Fractals*, vol. 12, no. 13, pp. 2427–2440, 2001.

[2] L. Walha, T. Fakhfakh, and M. Haddar, "Backlash effect on dynamic analysis of a two-stage spur gear system," *Journal of Failure Analysis and Prevention (JFAP)*, vol. 6, no. 3, pp. 60–68, 2006.

[3] H. Moradi and H. Salarieh, "Analisis of nonlinear oscillations in spur pairs with approximated modelling of backlash nonlinearity," *Mechanism and Machine Theory*, vol. 51, pp. 14–31, 2012.

[4] S. Wei, Q. Han K, and X. Dong J, "Dynami response of a single-mesh gear syatem with periodic mesh stiffness and backlash nonlinearity under uncertainty," *Nonlinear Dynamics*, vol. 89, no. 1, pp. 49–60, 2017.

[5] Z. Cao, Y. Shao, M. Rao, and W. Yu, "Effects of the gear eccentricities on the dynamic performance of a planetary gear set," *Nonlinear Dynamics*, vol. 91, pp. 1–15, 2018.

[6] J. Lu, H. Chen, F. Zeng, A. F. Vakakis, and L. A. Bergman, "Influence of system parameters on dynamic behavior of gear

pair with stochastic backlash," *Meccanica*, vol. 49, no. 2, pp. 429–440, 2014.

[7] J Lu, F Zeng, J Xin et al., "Influence of Stochastic Perturbation of Parameters on Dynamic Behavior of Gear System," *Journal of Mechanical Science and Technology*, vol. 25, no. 7, pp. 1667–1673, 2011.

[8] Q. Chen, Y Ma, S Huang et al., "Research on gears' dynamic performance influence by gear backlash based on fractal theory," *Applied Surface Science*, vol. 313, pp. 325–332, 2014.

[9] L. Yong, Natalie. Baddour, and L. Ming, "Effect of Gear Center Distance Variation on Time Varying Mesh Stiffness of a Spur Gear Pair," *Engineering Failure Analysis*, vol. 75, pp. 37–53, 2017.

[10] Y. S. Chen, Y. J. Tang, W. C. Lou et al., "Nonlinear dynamic characteristics of geared rotor bearing system with dynamic backlash and friction," *Mechanism and Machine Theory*, vol. 46, pp. 466–478, 2011.

[11] L. Xiang and N. Gao, "Coupled torsion–bending dynamic analysis of gear-rotor-bearing system with eccentricity fluctuation," *Applied Mathematical Modelling*, vol. 50, pp. 569–584, 2017.

[12] J. H. Kuang and Y. T. Yang, "An estimate of mesh stiffness and load sharing ratio of a spur gear pair," in *Proceedings of the International Power Transmission and Gear Conference*, vol. 1, pp. 1–9, 1992.

[13] A. Kahraman and R. Singh, "Interactions between time-varying mesh stiffness and clearance non-linearities in a geared system," *Journal of Sound and Vibration*, vol. 146, no. 1, pp. 135–156, 1991.

[14] C. Siyu, T. Jinyuan, L. Caiwang, and W. Qibo, "Nonlinear dynamic characteristics of geared rotor bearing systems with dynamic backlash and friction," *Mechanism and Machine Theory*, vol. 46, no. 4, pp. 466–478, 2011.

[15] Y. Luo, N. Baddour, and M. Liang, "Effects of gear center distance variation on time varying mesh stiffness of a spur gear pair," *Engineering Failure Analysis*, vol. 75, pp. 37–53, 2017.